Appl. Phys. B 91, 669–675 (2008)
DOI: 10.1007/s00340-008-2995-5

Applied Physics B
Lasers and Optics

M. LUONG[1,✉]
R. ZHANG[2]
C. SCHULZ[1]
V. SICK[2]

Toluene laser-induced fluorescence for in-cylinder temperature imaging in internal combustion engines

[1] IVG, University of Duisburg–Essen, Lotharstraße 1, 47057 Duisburg, Germany
[2] Department of Mechanical Engineering, University of Michigan, Ann Arbor, MI, USA

Received: 30 November 2007 /
Revised version: 19 February 2008
Published online: 22 April 2008 •

ABSTRACT A single-laser single-camera imaging technique was demonstrated for in-cylinder temperature distribution measurements in a direct-injection internal combustion engine. The single excitation wavelength two-color detection technique is based on toluene laser-induced fluorescence (LIF). Toluene-LIF emission spectra show a red-shift with increasing temperature. Temperature can thus be determined from the ratio of the signal measured in two separate wavelength ranges independent of the local tracer concentration, laser pulse energy, and the intensity distribution. An image doubling and filtering system is used for the simultaneous imaging of two wavelength ranges of toluene LIF onto the chip of a single camera upon excitation at 248 nm. The measurements were performed in a spark-ignition engine with homogeneous charge and yielded temperature images with a single-shot precision of approximately $\pm 6\%$.

PACS 32.50.+d; 42.62.-b; 47.80.Fg

1 Introduction

Detailed knowledge of in-cylinder mixture formation and combustion is crucial for the development of modern combustion engines with high efficiency and low pollutant emissions. Local mixture conditions, equivalence ratio and exhaust gas fraction, along with the temperature before ignition largely determine the performance of an engine. Therefore, it is important to experimentally determine quantities like fuel and air concentration as well as temperature and use this information either in engine development programs or towards the development and validation of advanced computational tools for engine design.

One way of gathering these quantities is laser-induced fluorescence (LIF) imaging in an optically accessible engine. The physical principle of this method is the electronic excitation of tracer molecules (e.g. toluene) by laser light and the detection of their subsequent fluorescence by a camera. Commercial fuels contain a variety of fluorescent molecules. The photophysical properties of these components in general are not well known and interaction of different fluorescence signals along with the ever varying composition of commercial fuels prevents quantitative interpretation. Thus, single fluorescing components are added to non-fluorescing fuel (e.g. aliphatic hydrocarbons) for quantitative measurements. The intensity of the LIF signal depends on pressure, temperature and local concentration of the tracer. The review article by Schulz and Sick [1] presents more details about the current state of tracer-LIF diagnostics in engine combustion systems. The work presented in this paper will exploit the temperature-dependent fluorescence intensity of toluene as a non-intrusive gas-phase imaging thermometer for in-cylinder measurements in IC engines.

Several approaches for fluorescence tracer-based thermometry have been presented in the past, taking advantage of temperature-dependent absorption and emission spectra [2–5]. The use of broadband absorbers such as organic molecules like ketones or aromatic molecules provides some advantages at higher pressures and temperatures in that the spectra are much broader than the line width of the exciting laser and therefore temperature and pressure-dependent overlap integrals do not have to be considered. This, however, is necessary when using small molecules such as nitric oxide or hydroxyl radicals as a temperature indicator [6, 7].

For homogeneous concentration distributions of the fluorescent tracer, temperature can be determined after single-line excitation from the signal intensity measured in a single wavelength band. The signal strength is a unique function of gas density and the known total temperature-dependent fluorescence yield so that a single-point calibration will allow quantitative measurements of temperatures [2, 4]. During the mixing phase in engine environments, however, the tracer distribution is not spatially homogeneous and the signal depends on local tracer number density and temperature at the same time. Thus, temperature is not accessible via a single-line measurement.

In LIF thermometry with two excitation wavelengths using ketones (i.e. 3-pentanone [8, 9] or acetone [2]) the restriction to homogeneous spatial tracer distributions is overcome by measuring the LIF signal ratio after exciting at two wavelengths where the LIF signal intensity shows a different temperature dependence. Here, the local tracer concentration cancels as long as the two different excitation wavelengths are used quasi-simultaneously (i.e. with a short time delay to separate the respective signals that are detected in the same wavelength interval via a 50/50 beam splitter or by observation from different angles). This had been demonstrated

✉ Fax: +49-203-379-3087, E-mail: myyen.luong@uni-due.de

for 3-pentanone tracer by Einecke et al. [3] and Fujikawa et al. [10] using toluene. In both cases, the measured temperature fields were used to process the initial LIF images to obtain quantitative concentration distributions.

In contrast to two-excitation-line thermometry [2, 9] the measurement technique described here uses a single excitation wavelength only. Kakuho et al. [11] have measured the temperature distribution in an HCCI engine with a single light source, using two types of fluorescent tracer (3-pentanone and triethylamine (TEA)). This single-excitation two-tracer method relies on the spectrally-separated fluorescence from the two tracers and the different temperature dependencies of their fluorescence signals. However, the assumption that quenching and temperature effects for TEA fluorescence signals are multiplicative has not been demonstrated in detail.

The single-excitation two-color detection technique based on toluene takes advantage of the temperature-dependent red-shift of the emission spectra [4] (Fig. 1). This technique has been demonstrated before for the determination of temperature distribution in mixing gas jets at atmospheric pressure [12, 13]. Again, the local tracer concentration $n_{\mathrm{tol}}(x, y)$ cancels for each pixel location (x, y). As an additional advantage, spatial variations in laser fluence $E_{\mathrm{laser}}(x, y)$ cancel in contrast to two-line excitation methods where the laser light sheet profile must be measured for each laser sheet. The intensities S_{fl} in the two spectral ranges can be detected simultaneously by using appropriate dichroic mirrors and bandpass filters. The signal intensity ratio is a function of temperature and both, local tracer concentration and laser fluence cancel at each point (x, y) in the images, thus

$$\frac{S_{\mathrm{fl}}^{\mathrm{red}}(x, y, T)}{S_{\mathrm{fl}}^{\mathrm{blue}}(x, y, T)} = \frac{\eta^{\mathrm{red}} E_{\mathrm{laser}}(x, y) n_{\mathrm{tol}}(x, y) \sigma_{\mathrm{abs}}(T(x, y)) \phi_{\mathrm{fl}}^{\mathrm{red}}(T(x, y))}{\eta^{\mathrm{blue}} E_{\mathrm{laser}}(x, y) n_{\mathrm{tol}}(x, y) \sigma_{\mathrm{abs}}(T(x, y)) \phi_{\mathrm{fl}}^{\mathrm{blue}}(T(x, y))} = c \frac{\phi_{\mathrm{fl}}^{\mathrm{red}}(T(x, y))}{\phi_{\mathrm{fl}}^{\mathrm{blue}}(T(x, y))} = f(T(x, y)) , \quad (1)$$

where σ_{abs} is the absorption cross-section, ϕ_{fl} the fluorescence quantum yield of the fluorescing species and η the detection efficiency for the respective wavelength band. The superscripts are used to distinguish between the two detection bandpasses ("blue" and "red").

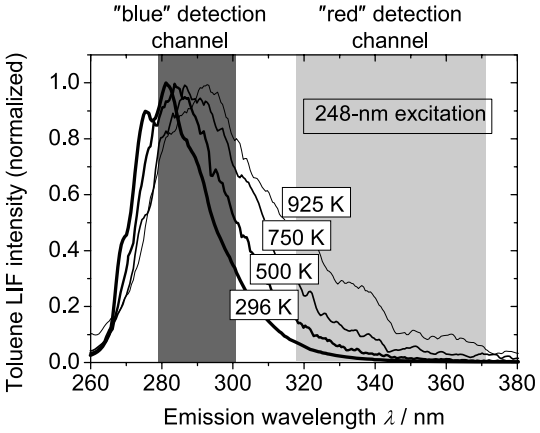

FIGURE 1 Red shift of the emissions spectrum with increasing temperature (adapted from [4])

The function $f(T)$ depends only on temperature as long as the oxygen partial pressure is at least 200 mbar. At lower O_2 partial pressure the toluene fluorescence emission spectra also depend on oxygen partial pressure [14] and therefore temperature can not be determined without knowing the local oxygen pressure.

The numerical values of $f(T)$ have been determined for the entire emission wavelength range in calibration experiments [4]. It must be noted that these measurements were performed at atmospheric pressure only. It was therefore assumed here that there is no additional pressure dependence that would vary with wavelength. Before applying $f(T)$ to extract temperature from measured fluorescence intensity ratios, a two-step calibration must be performed. First, the expected intensity ratio for the particular filter combination in use must be determined by multiplying the measured emission spectra with the filter transmission curves and integrating over the respective band pass. Second, potential differences in spectral sensitivity of the detector must be determined. A calibration measurement at known temperatures can accomplish this.

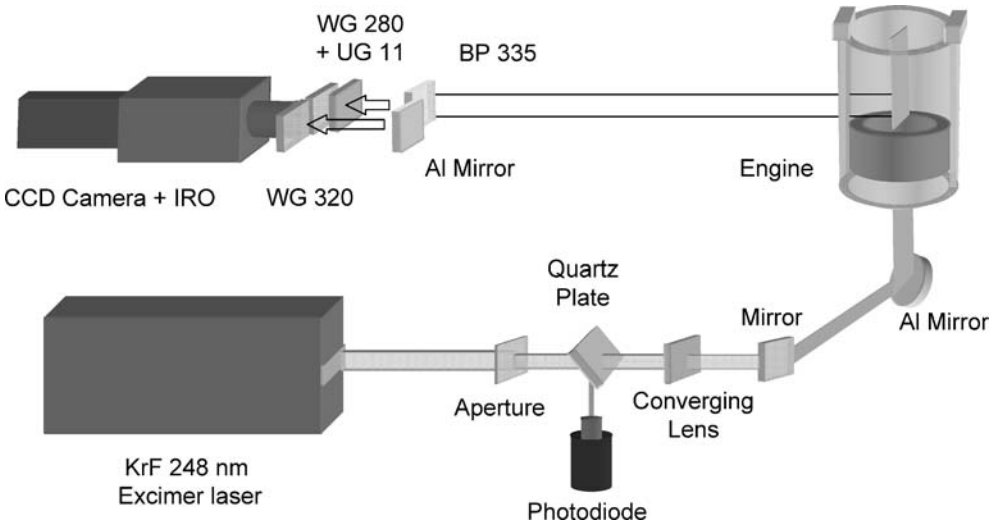

FIGURE 2 Schematic of the experimental setup

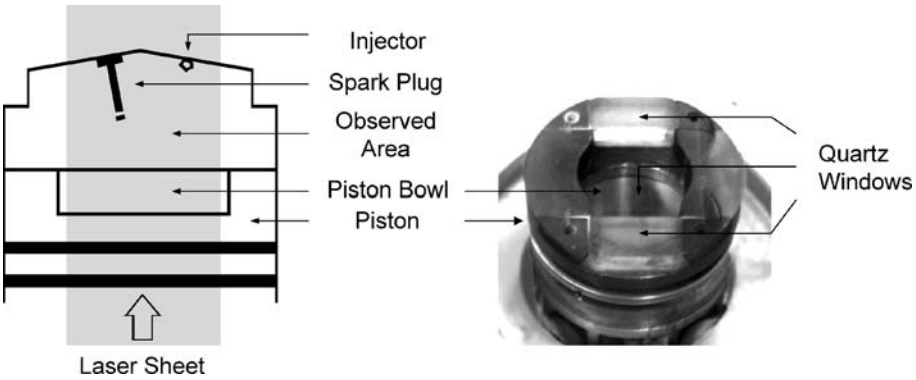

FIGURE 3 *Left*: Sketch of the laser sheet position and the observed area inside the cylinder. *Right*: Piston with a flat quartz crown window and two small side windows

2 Experimental

The temperature measurement technique was applied in a four-stroke spark-ignition engine with optical access to the chamber through a full-length quartz cylinder liner (see Smith and Sick [15] for details on the engine). Figure 2 shows the experimental setup. A broadband excimer laser (Lambda Physik COMPEX 102) operated at 248 nm (KrF*) was used as the excitation light source. Laser light was formed to a light sheet (0.5 mm thick, 35 mm wide, 17 mJ/pulse) which illuminated a vertical plane within the cylinder. The plane intersected the piston through its piston bowl and then the spark plug electrode and the injector tip. Spark plug and injector are inclined toward each other on the head. The center section of the piston bottom and two small windows on the side of the piston are made from quartz which allows for optical access into the bowl. The sectional drawing in Fig. 3 illustrates the laser sheet position and viewing area inside the cylinder. Figure 3 also displays the shape of the piston with its piston bowl. The signal was detected by a CCD camera (FlowMaster3S Imager Intense, LaVision) lens-coupled with an image intensifier unit (IRO, LaVision). On-line dark current subtraction was used for the camera. The image acquisition system was situated orthogonally to the plane of the laser light sheet in a position to capture the fluorescence through the side of the engine. The signal passed through an achromatic UV lens ($f = 100$ mm, $f_\# = 2$, Halle) onto the image intensifier. The filter setup was placed in front of the achromatic lens. In order to detect information from two spectral regions on a single camera a filter and mirror assembly [16, 17] was set up as shown in Fig. 2. A dielectric 45° mirror on a quartz substrate centered at 335 ± 45 nm was used to split the incident signals into two parts. The "red" (> 310 nm) portion of the spectrum was reflected, the "blue" (< 310 nm) region of the toluene-LIF emission spectrum was transmitted. An UV-enhanced aluminum mirror reflected the signal towards the camera. This allows simultaneous recording of "blue"/"red" image pairs on the same camera chip. Additional filters were used in both signal paths to further isolate the desired spectral ranges for each channel. For the "blue" channel a combination of a Schott WG 280 long-pass filter and a UG 11 filter cut off scattered laser light and reduced the interference by ambient light. In the "red" channel a Schott WG 320 long-pass filter suppressed scattered laser light as well as toluene fluorescence below 320 nm. The transmittance characteristics of the two imaging channels were measured by a fiber optic spectrometer system (Ocean Optics, USB 2000) and are shown in Fig. 4.

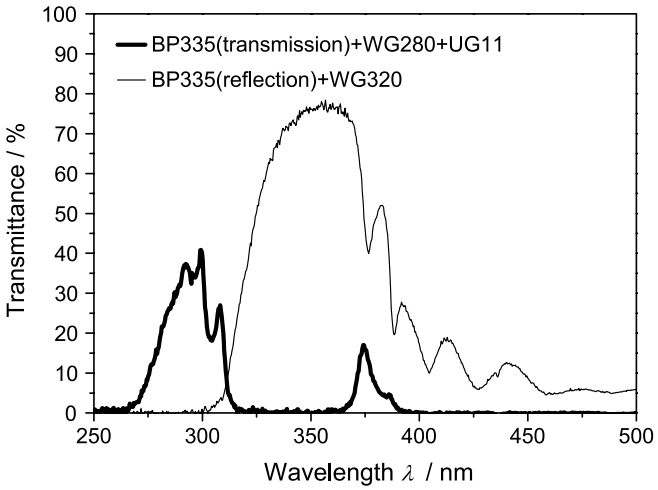

FIGURE 4 Transmittance curves for the filter assembly

Note that in experiments with commercial fuels wavelength-dependent signal absorption by fuel components or interfering fluorescence might bias the calibration curve; laser light attenuation is not important since the single line excitation strategy does not dependent on local laser energy. Even if absorbing or fluorescing compounds are not part of the fuel, they might be formed in pre-ignition chemistry (e.g. in HCCI combustion close to auto ignition).

The single-cylinder four-stroke spark-ignition direct-injection engine was operated at a speed of 2000 rpm. Oil and coolant were heated and stabilized to 95 °C and the intake manifold pressure was controlled at 95 kPa. A premixing unit was used to produce a homogeneous mixture of toluene and air that then was introduced into the intake air flow. During these experiments, the engine was motored without fuel injection. The convention used in this work is to refer to top-dead-center (TDC) at the beginning of the power stroke as 0° CAD and TDC at the beginning of the intake stroke as 360° before TDC.

Fluorescence images were taken from 40–90° CA after TDC. That late in the cycle, temperature inhomogeneities are expected to be lowest and thus, a baseline evaluation of the temperature measurement precision is best under those conditions.

Temperature reference images were recorded with the engine at rest. Intake and exhaust valves were opened simultan-

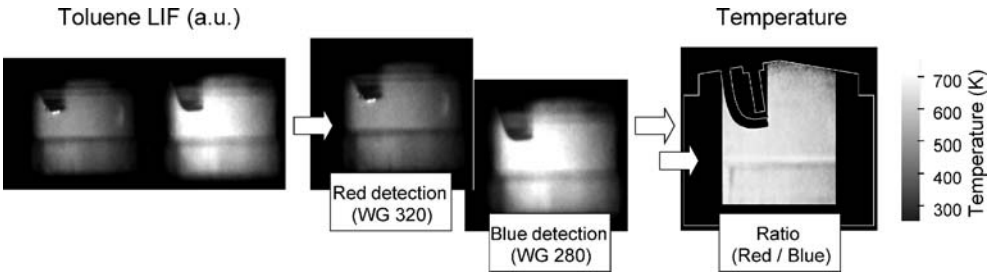

FIGURE 5 Simplified illustration of image processing. The ratio "red/blue" corrected a slight nonlinearity in the dependence on temperature

eously to flow a premixed fuel/tracer/air blend through the engine. The temperature of the gas under this condition could be monitored with thermocouples.

3 Data evaluation

Processing of the raw LIF images included a number of steps to ensure that any non-toluene-LIF background signals and spatial distortions are removed before calculating the intensity ratio. Figure 5 demonstrates this process. First, the raw LIF images were corrected for background scattering. The background images were captured for each crank angle where LIF images were taken by motoring the engine without adding tracer to the intake air while the laser was firing. Second, a 3×3 pixel spatial filter was applied to smooth all individual images for noise reduction. The signal from the two wavelength ranges is available as image pairs acquired simultaneously on the camera chip. Hence, each image was then split into two images which represent "red" and "blue" signals respectively. In the next step, the images were corrected for spatial distortion which is mainly caused by the detection optics. This was done by using images of a calibration plate (i.e. a grid with equidistant crosses on a flat plate). A correction routine integrated in the Davis (LaVision) software package was used to straighten and scale the corresponding images. The ratio $S_{\text{ratio}} = S_{\text{fl}}^{\text{red}} / S_{\text{fl}}^{\text{blue}}$ was calculated for each individual image pair resulting in a two-dimensional image where the signal intensity is a non-linear function of temperature.

Reference image pairs have been measured at known temperatures (368 and 296 K) and were used to normalize the measured two-color intensity ratio to the value that was given by $f(T)$ at those reference temperatures.

In order to determine temperatures from the resulting signal ratio a calibration curve was obtained from previous spectroscopic studies in a static cell [4]. The curve was calculated for the filter combination in use. The temperature-dependent toluene spectra were weighted with the filter transmissions for both detection wavelength ranges (Fig. 4) and then integrated over the respective detection bands. This produced the integrated signal that is expected for a given temperature. The calibration curve was fitted by:

$$\frac{S_{\text{fl}}^{\text{red}}}{S_{\text{fl}}^{\text{blue}}} = 2.6 \times 10^{-6} T^2 - 9.3 \times 10^{-5} T + 0.7\,, \quad \text{with } T \text{ in K}\,. \tag{2}$$

This function (Fig. 6) was then used to assign absolute temperatures to each pixel for the measured LIF ratio image. A mask was finally added to the images to highlight the significant area and to indicate the engine head profile and spark plug position.

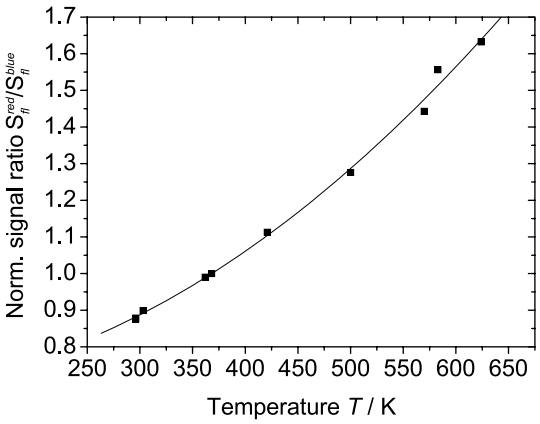

FIGURE 6 Fluorescence signal ratio as a function of temperature in an air environment. Signal ratio was normalized at 368 K

Note the horizontal streaks in the images in Fig. 5. Those mark the location of the piston top where signals are either blocked or additional signal is captured by the camera after reflection off the surface of the piston bowl side windows (see Fig. 3 for reference). It was therefore not expected that reliable temperature values would be obtained in this region of the images.

4 Results

Sets of 30 individual temperature distribution images per crank-angle degree and operating condition were obtained from the fluorescence measurements. These images were analyzed individually and as ensemble averages. Data from the expansion stroke were selected to illustrate the applicability of the single-excitation single-camera temperature measurement technique and to find the precision limitations under conditions with the lowest expected spatial temperature gradients.

Examples of single-shot temperature images are shown in Fig. 7 (top line). The examples shown in Fig. 7 (bottom line) illustrate the reduction in spatial noise by the ensemble-averaging over 30 individual temperature fields. The images show a high level of spatial homogeneity, though a slight gradient is noticed towards the cylinder wall in the right and the cylinder head on top of the images. The expected temperature drop with increasing crank angle is clearly captured. Note again the artifact that was introduced at the position of the piston side window location. It can be observed how the piston moves downward by following the horizontal streak in the image sequence.

An assessment of the precision of the temperature measurement can be made through a statistical analysis of the

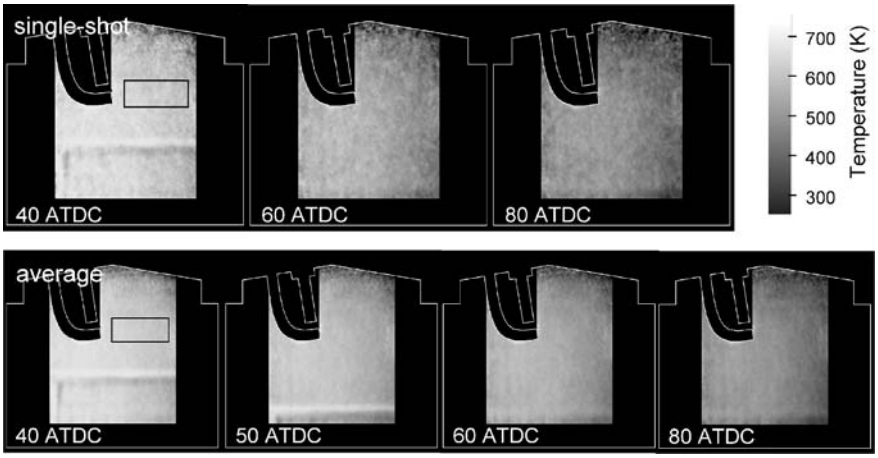

FIGURE 7 In-cylinder single-shot temperature distributions with homogeneous mixing of fuel and air (*top*). Each image is the ensemble average of 30 single-shot temperature images (*bottom*)

results. Mean and standard deviation results were obtained from temperature histograms. Those were assembled from data taken in a rectangular area ($4 \times 10\,\text{mm}^2$) near the spark plug in the center of the combustion chamber where near-adiabatic conditions can be assumed. The selected region is marked with a rectangle in some images shown in Fig. 7. Sample histograms for single-shot and ensemble-averaged temperatures are depicted in Fig. 8. The averaged temperatures (black bars) were computed from temperature fields taken in 30 cycles. The white bars show the single-shot temperature data points within the selected rectangle from all 30 images. The shape of the histograms is reasonably described by a normal (Gaussian) distribution so that means and standard deviations could be used in the conventional manner. Note that for the display in Fig. 8 the bin size was chosen to highlight the single-shot data. As a result, the ensemble-averaged data

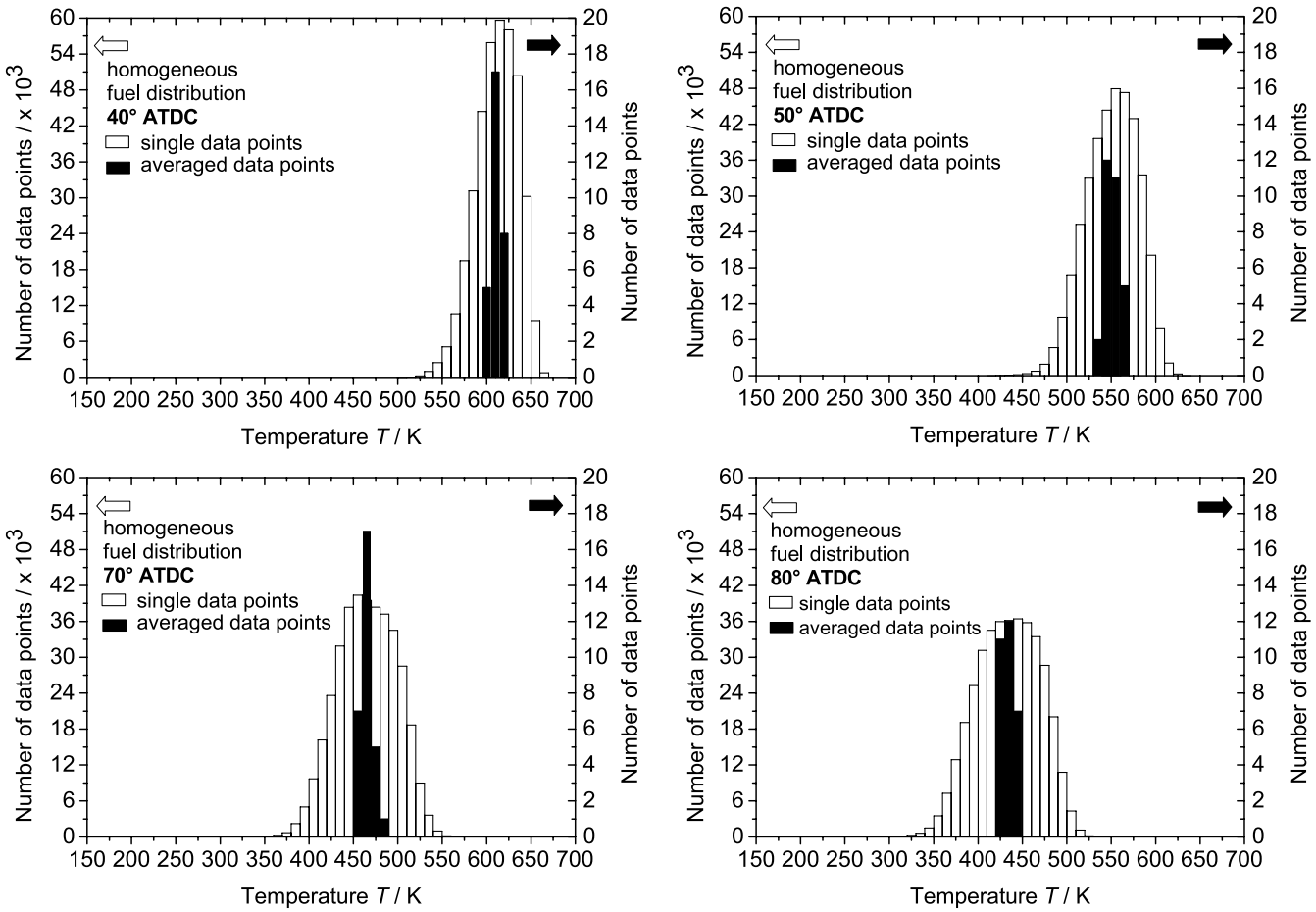

FIGURE 8 Histogram for temperatures at various example positions of the piston. The temperatures (*black bars*) used are the averaged temperatures from 30 images within the selected rectangle at each respective crank angle position. The *white bars* derived from single data points within the selected rectangle. Descriptions to the right of the bars refer to the averaged data points (*black bars*) and those to the left refer to the single data points (*white bars*)

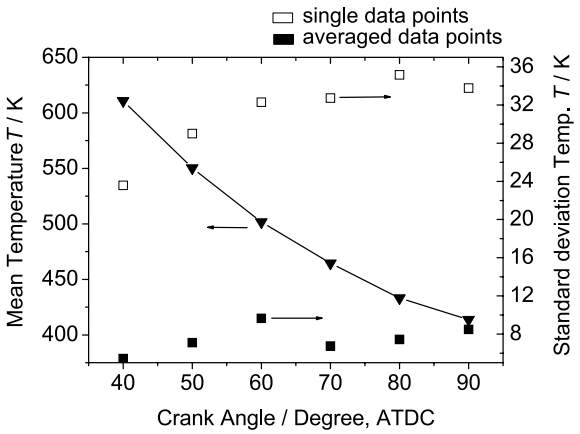

FIGURE 9 Measured mean temperatures (*black triangles*), standard deviation of single data points (*white squares*) and of averaged data points (*black squares*) vs. crank angle

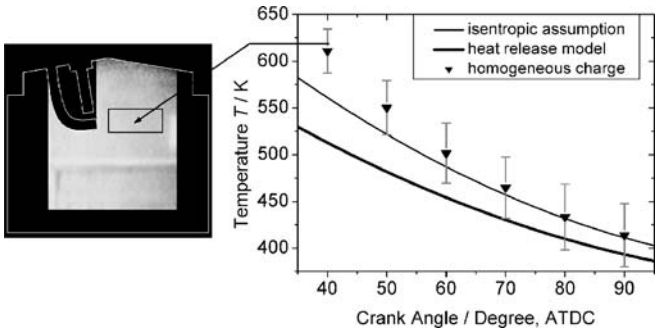

FIGURE 10 Comparison of measured and calculated temperatures derived from thermodynamic analysis

exhibits an apparent asymmetry due to the limited display resolution. The standard deviation of the temperatures derived from the single-shot data set increases from 40 to 90° CA after TDC from 24 to 34 K. For the ensemble averaged results the standard deviation shows no systematic variation with crank angle (see Fig. 9). It is important to note that the measured standard deviation of the temperature includes cycle-to-cycle variations in the engine and the statistical error of the measurement. The temperature measurements can be obtained with a (1σ) precision of ± 34 K for single-pulse measurements. This corresponds to a relative error of approximately 5.5% at 600 K. Ensemble-averaging improved this precision to ± 7 K which corresponds to 1.2% at 600 K. The reduction of the precision error by ensemble averaging follows exactly the expected $N^{1/2}$ relation where $N = 30$ in this case confirming that random noise is the source for limitations in measurement precision.

While every attempt was made here to address the temperature measurement precision as independent of engine operating conditions as possible, it has to be kept in mind that the reported precision values will include natural cycle-to-cycle variations and therefore do not fully show the real (lower) precision error of the measurement technique. A brief comparison to similar measurements that are reported in the literature will have to be interpreted in this context.

Fujikawa et al. [10] used toluene with two-excitation wavelengths (248 and 266 nm) to measure the temperature distributions in a SI engine both in PFI and DI operation prior to ignition. The precision of this technique is determined from a homogeneous PFI experiment. The standard deviation is within 5% for the average temperature, which is considered as the error of this technique if the temperature field is uniform. The accuracy to the adiabatic temperature is estimated as 8% at the maximum.

Einecke et al. [3] measured the instantaneous temperature distribution fields during the compression stroke and the unburned end-gas region of an optical two-stroke SI engine with a 3-pentanone two-wavelength excitation LIF technique. They selected the wavelengths which are located on opposite sides of the absorption maximum (248 and 308 nm) in order to reach a strong temperature dependence of the ratio, hence accuracy. For single-shot temperature measurements in the motored engine they obtained a precision of better than ± 17 K which corresponds to a relative error of approximately 4%.

The two-wavelength scheme based on 3-pentanone has higher temperature sensitivity (three times in the temperature range of 368–575 K) than the single-wavelength scheme based on toluene. This might lead to higher accuracy and precision if suitable referencing to the local laser intensities is implemented for the ketone-based technique. However, in practice, this might be extremely difficult especially when beam steering effects are present that could affect the laser intensity distribution of the two beams differently. The use of a single excitation wavelength eliminates the effect of temporal and spatial variations in laser beam intensity.

Figure 10 shows the experimental results in comparison to the calculations from thermodynamic analysis of measured in-cylinder pressures. The upper limit of the expected temperature range is set by assuming isentropic compression starting from intake valve closing (IVC). An analysis using a heat release model that includes the option of heat and mass transfer [18] produces somewhat lower temperatures.

Deviations between measured and pressure-derived temperatures increase with increasing temperature. While still within a 2σ uncertainty limit to the isentropic temperature it is also reasonable to assume that the temperature in the core of the in-cylinder volume should be higher than the bulk average temperature. The cylinder walls, piston surface, and cylinder head are all at a significantly lower temperature and therefore a gradient, at least qualitatively similar to what is observed in Fig. 7 could be expected.

5 Conclusions and future work

A single-wavelength excitation two-color detection toluene-LIF imaging technique was applied for the first time to measure in-cylinder temperature distributions in a motored optical spark-ignition direct-injection engine. Application will be feasible for fired engine operation and would provide temperature information for unburned regions. The simultaneous measurement of two spectral ranges of toluene LIF allowed the determination of temperature distributions without the need for corrections for variations in laser pulse energy, light sheet intensity, and local tracer concentration. Measurements were performed using a broadband KrF* excimer laser and a single image-intensified CCD camera that was coupled with a combined image splitter/filter unit. Using

the spectral calibration data from Koban et al. [4] and measured filter transmission data, a function was determined that uniquely linked the measured fluorescence intensity ratio from two spectral bandpasses to temperature. Measurements were performed for a premixed operation of a motored single cylinder engine to define the precision limits for single-shot and ensemble-averaged temperature distribution measurements. A 1σ temperature measurement precision of ± 34 K was obtained for single-pulse measurements. Ensemble-averaging improved this precision to ± 7 K.

ACKNOWLEDGEMENTS Funding by the Deutsche Forschungsgemeinschaft (DFG) and by the General Motors Corporation is gratefully acknowledged. The authors thank also the Deutscher Akademischer Austauschdienst (DAAD) for financial support. R.Z. and V.S. were supported by General Motors within the GM-UM-Collaborative Research Laboratory on Engine Systems Research.

REFERENCES

1 C. Schulz, V. Sick, Prog. Energ. Combust. Sci. **31**, 75 (2005)
2 M.C. Thurber, F. Grisch, R.K. Hanson, Opt. Lett. **22**, 251 (1997)
3 S. Einecke, C. Schulz, V. Sick, Appl. Phys. B **71**, 717 (2000)
4 W. Koban, J.D. Koch, R.K. Hanson, C. Schulz, Phys. Chem. Chem. Phys. **6**, 2940 (2004)
5 D.L. Peterson, F.E. Lytle, N.M. Laurendeau, Appl. Opt. **27**, 2768 (1988)
6 J.M. Seitzman, R.K. Hanson, P.A. deBArber, C.F. Hess, Appl. Opt. **33**, 4000 (1994)
7 A.O. Vyrodov, J. Heinze, M. Dillmann, U.E. Meier, A.W. Stricker, Appl. Phys. B **61**, 409 (1995)
8 F. Grossmann, P.B. Monkhouse, M. Ridder, V. Sick, J. Wolfrum, Appl. Phys. B **62**, 249 (1996)
9 J.D. Koch, R.K. Hanson, Appl. Phys. B **76**, 319 (2003)
10 T. Fujikawa, K. Fukui, Y. Hattori, K. Akihama, SAE Tech. Paper Series 2006-01-3336 (2006)
11 A. Kakuho, M. Nagamine, Y. Amenomori, T. Urushihara, T. Itoh, SAE Technical Paper Series 2006-01-1202 (2006)
12 M. Luong, W. Koban, C. Schulz, Novel strategies for imaging temperature distribution using Toluene LIF (Int. Conf. on Laser Diagnostics, ICOLAD2005, London, 2005, J. of Phys.: Conf. Series 45)
13 F. Zimmermann, W. Koban, C. Schulz: Temperature diagnostics using laser-induced fluorescence (LIF) of toluene (Laser Applications to Chemical Security and Environmental Analysis 2006 Tech. Digest. Opt. Soc. Amer., Washington, DC, 2006, TuB4)
14 W. Koban, J.D. Koch, R.K. Hanson, C. Schulz, Appl. Phys. B **80**, 147 (2005)
15 J.D. Smith, V. Sick, Appl. Phys. B **81**, 579 (2005)
16 B.D. Stojkovic, V. Sick, Appl. Phys. B **73**, 75 (2001)
17 R. Zhang, N. Wermuth, V. Sick, SAE Tech. Paper Series 2004-01-2975 (2004)
18 W. Koban, J.D. Koch, V. Sick, N. Wermuth, R.K. Hanson, C. Schulz, Proc. Combust. Inst. **30**, 1545 (2005)